Report

Cell Reports

Peroxiredoxin 1 Protects Telomeres from Oxidative Damage and Preserves Telomeric DNA for Extension by Telomerase

Graphical Abstract

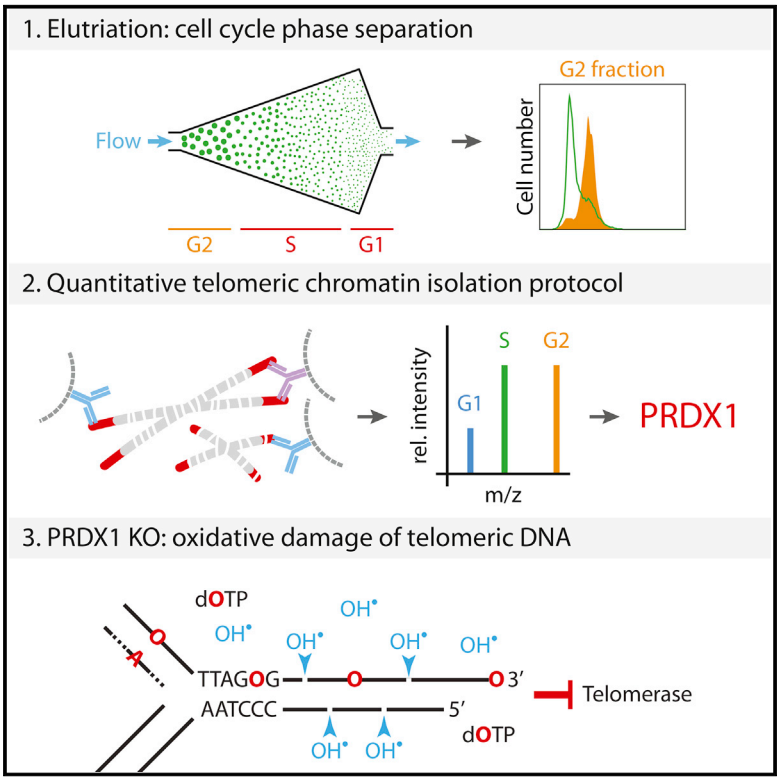

Highlights

- The antioxidant enzyme PRDX1 associates with telomeric chromatin
- PRDX1 protects telomeres from oxidative damage
- Oxidized telomeric DNA cannot be extended by telomerase

Authors

Eric Aeby, Wareed Ahmed, Sophie Redon, Viesturs Simanis, Joachim Lingner

Correspondence

joachim.lingner@epfl.ch

In Brief

Aeby et al. analyze the protein composition of telomeres during the cell cycle. The antioxidant enzyme PRDX1 associates with telomeres during S and G2 phases of the cell cycle. Deletion studies reveal that PRDX1 protects telomeres from acute oxidative damage. Oxidized telomeric DNA cannot be extended by telomerase.

Accession Numbers

PXD002626

Aeby et al., 2016, Cell Reports *17*, 3107–3114
December 20, 2016
http://dx.doi.org/10.1016/j.celrep.2016.11.071

Cell Reports
Report

Peroxiredoxin 1 Protects Telomeres from Oxidative Damage and Preserves Telomeric DNA for Extension by Telomerase

Eric Aeby,[1,2,3,4] Wareed Ahmed,[1,2] Sophie Redon,[1] Viesturs Simanis,[1] and Joachim Lingner[1,5,*]
[1]Swiss Institute for Experimental Cancer Research (ISREC), School of Life Sciences, Ecole Polytechnique Fédérale de Lausanne (EPFL), 1015 Lausanne, Switzerland
[2]Co-first author
[3]Present address: Department of Molecular Biology, Massachusetts General Hospital, Boston, MA 02114, USA
[4]Present address: Department of Genetics, Harvard Medical School, Boston, MA 02114, USA
[5]Lead Contact
*Correspondence: joachim.lingner@epfl.ch
http://dx.doi.org/10.1016/j.celrep.2016.11.071

SUMMARY

Oxidative damage of telomeres can promote cancer, cardiac failure, and muscular dystrophy. Specific mechanisms protecting telomeres from oxidative damage have not been described. We analyzed telomeric chromatin composition during the cell cycle and show that the antioxidant enzyme peroxiredoxin 1 (PRDX1) is enriched at telomeres during S phase. Deletion of the *PRDX1* gene leads to damage of telomeric DNA upon oxidative stress, revealing a protective function of PRDX1 against oxidative damage at telomeres. We also show that the oxidized nucleotide 8-oxo-2′deoxyguanosine-5′-triphosphate (8oxodGTP) causes premature chain termination when incorporated by telomerase and that some DNA substrates terminating in 8oxoG prevent extension by telomerase. Thus, PRDX1 safeguards telomeres from oxygen radicals to counteract telomere damage and preserve telomeric DNA for elongation by telomerase.

INTRODUCTION

With the increase of atmospheric oxygen 2.3 billion years ago, cells evolved mechanisms to mitigate the toxic effects of oxygen radicals, which damage nucleic acids, proteins, and lipids. The cell's armory of antioxidant enzymes includes the peroxidases catalase, glutathione peroxidases, and peroxiredoxins, which reduce a large fraction of cellular peroxides (Perkins et al., 2015). Oxidative stress has been reported to accelerate the telomere shortening (Ahmed et al., 2008; von Zglinicki, 2002) that occurs in every round of DNA replication in the absence of telomerase and ultimately promotes cellular senescence (Forsyth et al., 2003). There are a number of reasons why telomeres are particularly vulnerable to oxidative damage. First, in order to safeguard overall chromosome structure, DNA damage signaling and DNA double-strand repair pathways are suppressed locally at telomeres; this is important to prevent the telomere being treated as a broken chromosome end, which could result in chromosome rearrangements (Fumagalli et al., 2012; Sfeir and de Lange, 2012). In this context, it is noteworthy that in addition to damaging DNA bases, oxidative stress can also lead to DNA strand breaks. Second, in vitro studies have shown that the 5′-GGG-3′ sequence in the 5′-TTAGGG-3′ telomeric DNA repeats is more prone to oxidation than other DNA sequences (Oikawa and Kawanishi, 1999). Third, telomeres contain single stranded DNA either at the chromosome 3′ end or internally at the displacement loop, which forms when the 3′ overhang invades the double-strand telomeric DNA sequences in the T-loop configuration (Doksani et al., 2013). The bases in the single-stranded region are not protected by hydrogen bonding to the other strand, and they cannot be repaired by base excision repair, which requires a complementary strand to provide a template for the replacement of damaged nucleotides. Currently, however, it is unclear how telomeres are protected from oxidative damage in vivo.

Using the recently developed quantitative telomeric chromatin isolation protocol (QTIP) approach (Grolimund et al., 2013), we show in this study that the antioxidant enzyme peroxiredoxin 1 (PRDX1) (Chae et al., 1994; Perkins et al., 2015) is enriched at telomeres in S and G2 phases of the cell cycle when telomeres are replicated. We demonstrate that PRDX1 reduces oxidative damage caused by reactive oxygen species (ROS) specifically at telomeres and that telomerase cannot efficiently elongate ROS-damaged telomeric DNA substrates. Together, the data presented here uncover a mechanism that reduces telomere damage, thereby delaying the onset of aging and fatal diseases.

RESULTS AND DISCUSSION

Identification of PRDX1 at Telomeres

As telomeres are difficult to replicate and susceptible to DNA damage (Miller et al., 2006; Sfeir et al., 2009; Vannier et al., 2012; von Zglinicki, 2002), we reasoned that they may compensate for their enhanced vulnerability by recruiting proteins that

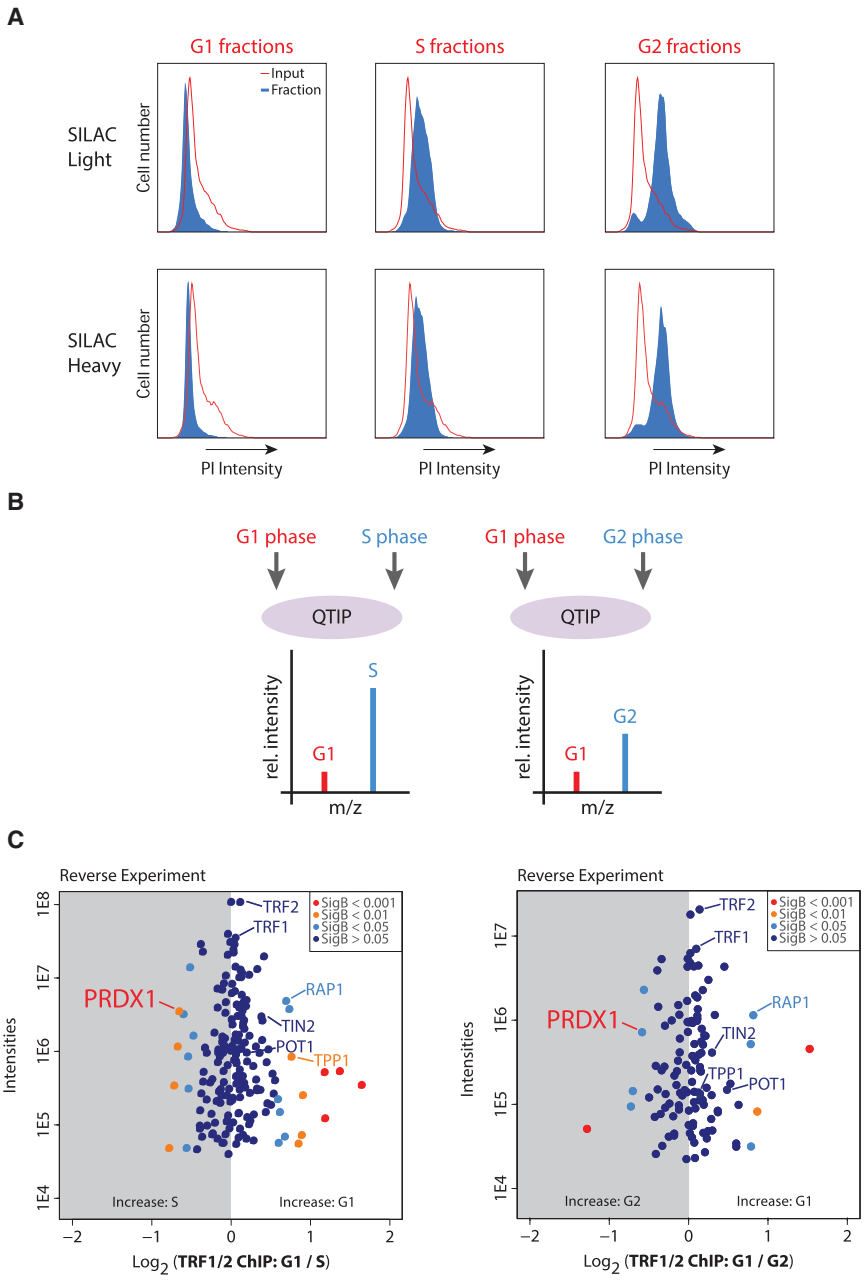

Figure 1. Identification of PRDX1 as a Cell-Cycle-Regulated Telomeric Protein by QTIP

(A) Representative flow cytometry profiles of cell fractions collected for QTIP.

(B) Workflow during QTIP. The same G1 cells were mixed with S or G2 phase cells for TRF1 and TRF2 immunoprecipitations. In red and blue, cell growth in different SILAC medium is indicated. Identical peptide fragments obtained from the differently labeled cells will differ in their mass to charge ratio. Differences in intensity reveal differences in abundance.

(C) Scatterplots showing $\log_2$ ratios of proteins at telomeres in G1/S and G1/G2 phases. Significance of differences in ratios is color-coded. Shelterin proteins and PRDX1 are highlighted. PRDX1 is increased at telomeres in S and G2 phase cells over G1. RAP1 and TPP1 were more abundant in G1 telomeric chromatin in the reverse, but not the forward, experiment (Figure S2).

See also Figures S1 and S2.

facilitate their replication or protect them from chemical damage. Therefore, we examined changes in the telomere-associated proteome during the cell cycle. HEK293E cells were grown in suspension cultures in either light or heavy stable isotope labeling with amino acids in cell culture (SILAC) medium, permitting quantitative comparison of the proteins of the two cultures by mass spectrometry (Ong and Mann, 2007). Chromatin was crosslinked with formaldehyde and ethylene glycol bis(succinimidyl succinate), and cells were fractionated by elutriation (Banfalvi, 2008) into cell populations that were in G1, S, and G2 phases of the cell cycle (Figure 1A; Figures S1A and S1B). G1 and S phase or G1 and G2 phase cells labeled with different SILAC media were mixed (Figure 1B), and telomeric chromatin was purified by QTIP (Grolimund et al., 2013; Majerska et al., 2016), which separates telomeric chromatin from total chromatin using antibodies against the shelterin components TRF1 and TRF2. Successful enrichment of telomeric chromatin was confirmed by quantifying telomeric DNA over Alu-repeat DNA in the chromatin fractions by Southern hybridization (Figure S1C). Telomeric chromatin fractions were digested with trypsin and analyzed by liquid chromatography-tandem mass spectrometry (LC MS/MS). In separate experiments, the G1 cells had been labeled either with light (reverse experiment, Figure 1C) or heavy (forward experiment, Figures S2A and S2B) SILAC medium and mixed with S or G2 cells grown in the opposite SILAC medium. Comparison of G1 to S and G1 to G2 telomeric chromatin-associated proteome did not reveal striking differences in shelterin protein abundance at telomeres. Strikingly, we obtained a very strong signal for PRDX1 in telomeric chromatin, and its abundance at telomeres was increased in S and G2 phases of the cell cycle over G1 in both the forward and reverse experiments (Figure 1C; Figures S2C and S2D). In addition, we identified PRDX2 and several DNA replication factors enriched in telomeric chromatin during S phase, whereas others were enriched at telomeres in G1 (Figure S2E).

To confirm association of PRDX1 with telomeres, we expressed triple hemagglutinin (HA)-epitope-tagged PRDX1 in HEK293T cells. N- and C-terminally tagged PRDX1 as well as endogenous PRDX1 were detected on western blots with anti-PRDX1 antibody, which showed similar expression levels of

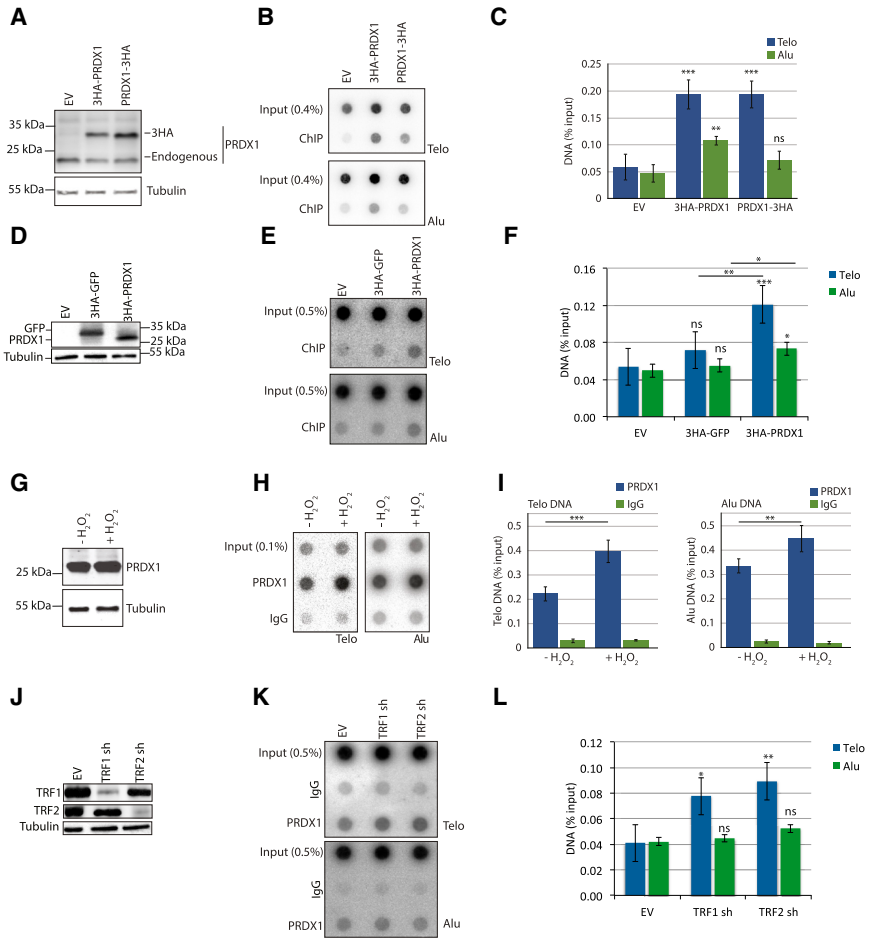

Figure 2. Validation of PRDX1 as a Telomeric Protein

(A) Immunoblot analysis of 3xHA-tagged PRDX1 expression. EV, 3xHA empty vector; 3HA-PRDX1, N-terminally tagged PRDX1; PRDX1-3HA, C-terminally tagged PRDX1. Tubulin was used as a loading control.

(B) ChIP analysis of 3xHA-tagged PRDX1. ChIPed DNA was probed with a telomere-specific probe (Telo) and for Alu-repeat DNA (Alu).

(C) Quantification of (B). Error bars correspond to SD from three independent experiments (unpaired t test, two-tailed p value, comparison to corresponding EV: ***$p < 0.005$, **$p < 0.05$).

(D) Immunoblot analysis of 3xHA-tagged GFP and 3xHA-tagged PRDX1 expression. EV, 3xHA empty vector; 3xHA-GFP, N-terminally tagged GFP; 3HA-PRDX1, N-terminally tagged PRDX1. Tubulin was used as a loading control.

(E) ChIP analysis of 3xHA-tagged GFP and PRDX1. ChIPed DNA was probed with a telomere-specific probe (Telo) and for Alu-repeat DNA (Alu).

(F) Quantification of (E). Error bars represent SD, and statistical analysis is as in (C).

(G) Immunoblot analysis of endogenous PRDX1 upon H_2O_2 treatment.

(H) Association of endogenous PRDX1 with telomeres analyzed by ChIP upon H_2O_2 treatment.

(I) Quantification of ChIP experiment in (H). Error bars represent SD, and statistical analysis is as in (C).

(J) Immunoblot analysis of the short-hairpin-RNA-mediated depletion of TRF1 and TRF2 in HeLa Long (HeLa L) cells, which contain telomeres with an average length of 33kb. EV, pSuper puro empty vector; TRF1 sh, short hairpin RNA against TRF1 transcript; TRF2 sh, short hairpin RNA against TRF2 transcript. Tubulin was used as a loading control.

(K) ChIP analysis of endogenous PRDX1 in TRF1- and TRF2-depleted HeLa L cells. ChIPed DNA was probed with a telomere-specific probe (Telo) and for Alu-repeat DNA (Alu). Similar results were obtained with HeLa cells containing an average telomere length of 11 kb.

(L) Quantification of (K). Error bars represent SD, and statistical analysis is as in (C).

endogenous and tagged proteins (Figure 2A). Association of HA-tagged PRDX1 with telomeric and Alu-repeat DNA was detected upon chromatin immunoprecipitation (ChIP) with anti-HA antibodies (Figures 2B–2F). N- and C-terminally HA-tagged PRDX1 associated with telomeric DNA; N-terminally tagged PRDX1 also associated with Alu-repeat DNA to a lesser extent. PRDX1 association with telomeric DNA was also seen in ChIP experiments using an anti-PRDX1 antibody whose specificity was confirmed in *PRDX1*-knockout cells (see below). Treatment of cells with 6.25 mM H_2O_2 for 3 hr prior to ChIP with anti-PRDX1 antibodies enhanced the telomeric DNA signal 2-fold and the signal for Alu-repeats to a lesser extent (1.3-fold; Figures 2G–2I). This indicates that oxidative stress promotes association of PRDX1 with chromatin. Depletion of TRF1 or TRF2 with short hairpin RNAs (shRNAs) increased the fraction of telomeric DNA, but not Alu-repeats, associated with PRDX1 in the ChIP experiments. These results suggest that PRDX1 is recruited to chromatin by factors other than shelterin. The increased association with the telomere in the absence of the core shelterin components may result from the DNA damage response due to the opening up of the telomere; future studies will examine this.

PRDX1 Protects Telomeres from Oxidative Damage

To investigate the importance of PRDX1 for telomeres, we disrupted the *PRDX1* genes in HT1080 fibrosarcoma and HCT116 colon cancer cells using clustered regularly interspaced short palindromic repeats (CRISPR)/Cas9 technology (Figure S3A). In order to exclude off-target effects, the cells were transfected in separate experiments with two different guiding RNAs. Cells were cloned and analyzed for loss of PRDX1 expression by western blot analysis (Figure 3A). Sequencing of *PRDX1* loci in cell clones revealed frameshift mutations causing premature stop codons explaining loss of PRDX1 expression (Figure S3A). Cell clones were characterized for telomere length (Figure S3B) and used to confirm the specificity of the PRDX1 antibody, which precipitated telomeric chromatin and, to a lesser extent, Alu repeats (Figure S3C). Importantly, the analysis of *PRDX1*-knockout clones did not reveal increased damage of telomeres or striking telomere length changes

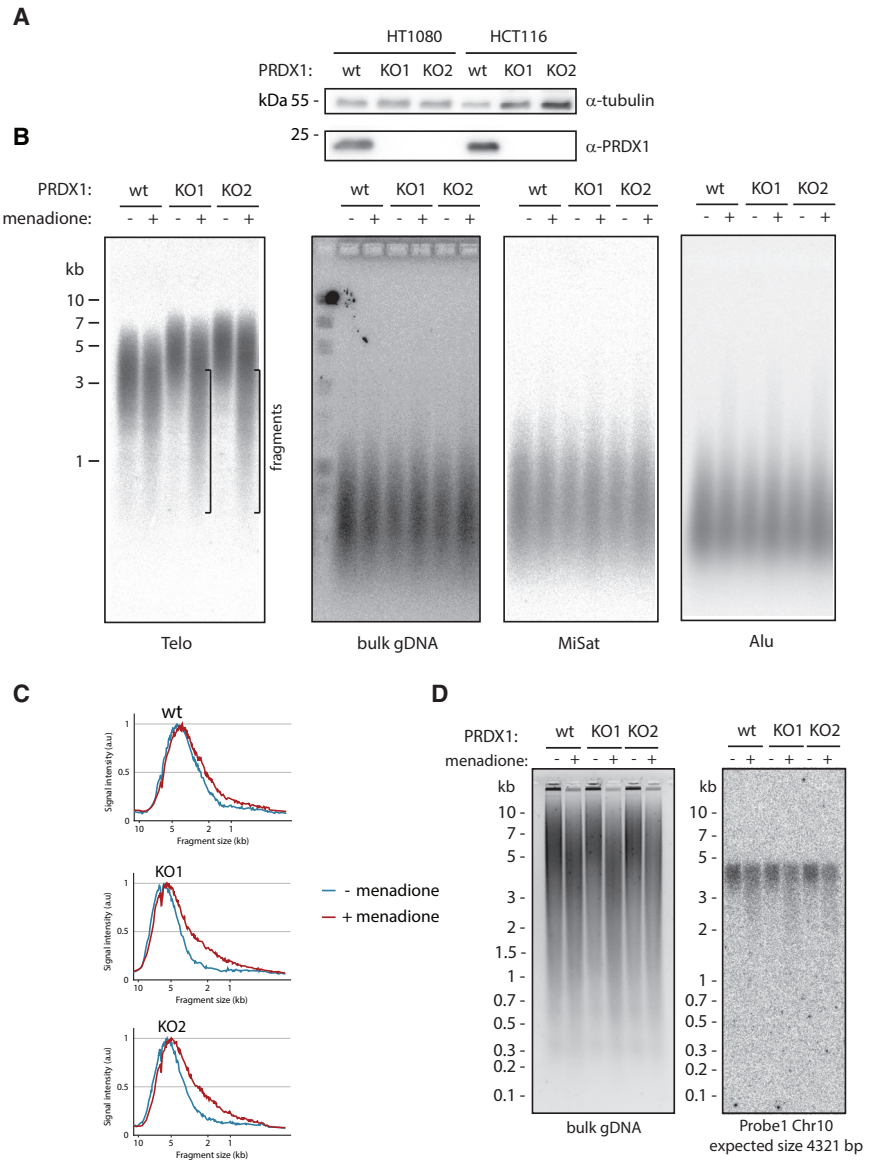

Figure 3. PRDX1 Protects Telomeres from Oxidative Damage

(A) Western blot analysis of wild-type (wt) and HT1080 and HCT116 *PRDX1*-knockout clones with anti-PRDX1 antibodies. Total cell extracts were loaded. Tubulin was detected as a loading control.

(B) Southern blot analysis of genomic DNA that was digested with HinfI/RsaI and resolved on denaturing alkaline gels (bulk gDNA). The membrane was sequentially probed for telomere (Telo), microsatellite (MiSat), and Alu-repeat DNA. Telomeric DNA fragments that accumulate in the *PRDX1*-knockout cells upon menadione treatment are indicated.

(C) Quantification of signal intensity profiles of Figure 3B (Telo panel).

(D) Southern blot analysis as in (B) except that DNA was digested with EcoRI. The blot was probed with a 4.3-kb region (coordinates: 72555–76876) of chromosome 10.

See also Figures S3 and S4.

upon propagation under standard unperturbed growth conditions (data not shown).

To test whether PRDX1 protects telomeres from acute oxidative stress, we incubated *PRDX1*-knockout clones and wild-type cells with 1 mM menadione for 30 min, which increases ROS (Loor et al., 2010). Genomic DNA was then isolated and digested with restriction enzymes, followed by analysis on denaturing alkaline agarose gels to separate the DNA strands and detect DNA backbone cleavage events (Figure 3B). The detection of telomeric DNA by Southern hybridization revealed that menadione treatment caused a significant increase of smaller telomeric DNA fragments in *PRDX1*-knockout clones indicative of DNA cleavage events (Figures 3B and 3C; Figure S4). In striking contrast, menadione-treatment did not markedly increase telomere damage in wild-type cells (Figures 3B and 3C; Figure S4). These findings support the notion that PRDX1 protects telomeres from acute oxidative stress. To address whether PRDX1 has a general role in protecting genomic DNA from oxidative stress, we stained the same gels with ethidium bromide and probed it consecutively for a microsatellite repeat ($5'$-$(TG)_n$-$3'$) and Alu-repeat DNA that have either the same (microsatellite) or higher (Alu repeats) GC content, respectively, than telomeres. No effects of loss of PRDX1 were observed, though the small restriction fragment sizes obtained using the 4-bp recognizing enzymes HinfI and RsaI may have reduced the sensitivity of the assay for these genomic regions. Therefore, we repeated the experiment with a 6-bp cutter and analyzed both a specific locus on chromosome 10 (GC content: 46.6%) and bulk genomic DNA (Figure 3D). This analysis showed that menadione triggered damage in total DNA and at the specific locus on chromosome 10 but *PRDX1* deletion did not enhance this damage. Taken together, these experiments support the notion that PRDX1 has specific functions to protect telomeres from oxidative damage. However, while the control locus on chromosome 10 and bulk of genomic DNA are not protected from oxidative damage by PRDX1, our data do not exclude the possibility that PRDX1 also functions at specific sites elsewhere in the genome.

Inhibition of Telomerase by ROS-Damaged Substrates

Oxidative damage has been reported to cause telomere shortening, and telomerase is also thought to be a target of ROS (Ahmed et al., 2008; Haendeler et al., 2003). The data presented above reveal conditions under which ROS cause oxidative damage and fragmentation of telomeric DNA that telomerase may

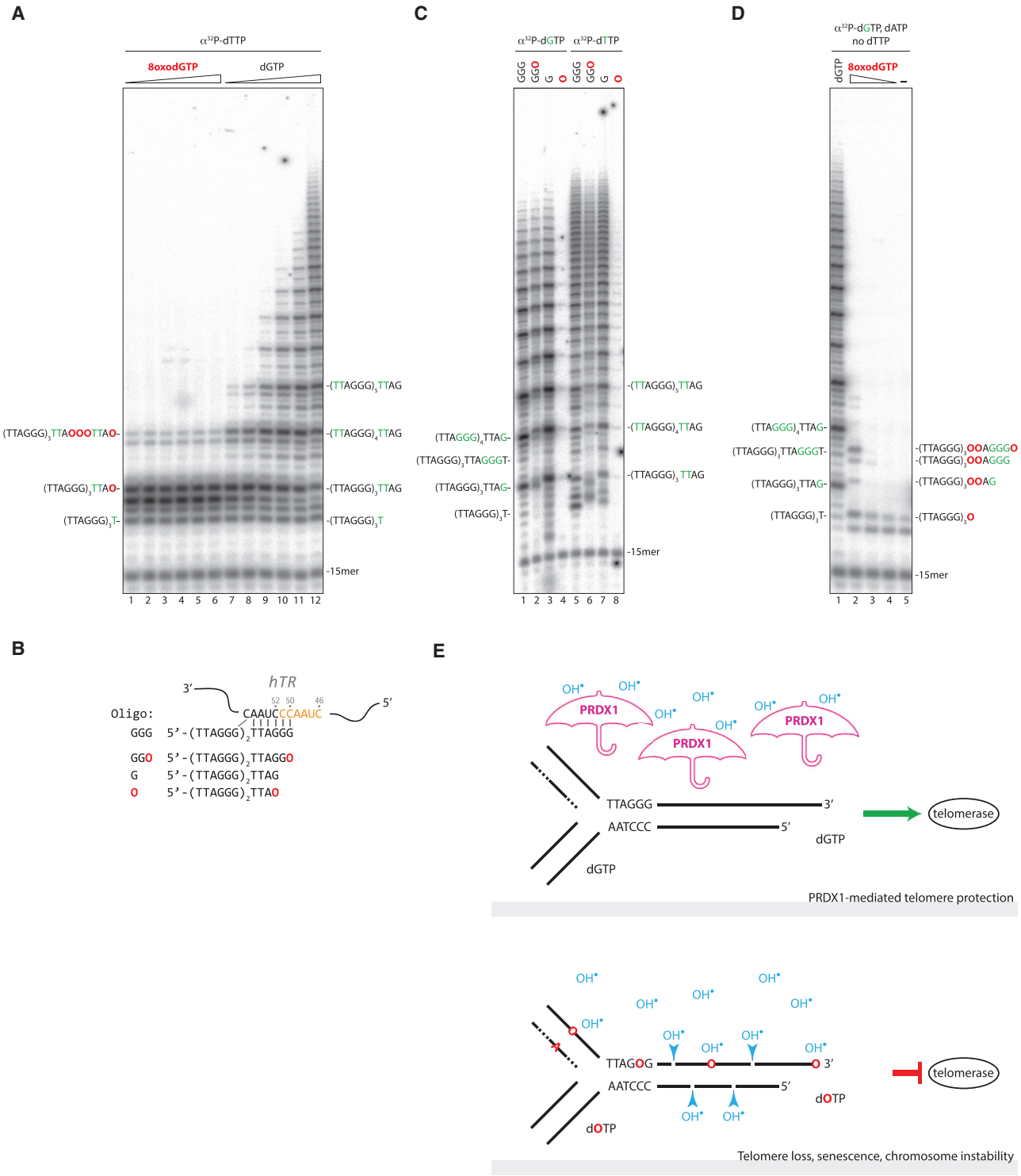

Figure 4. Oxidative DNA Damage Inhibits Telomerase Activity

(A) Direct telomerase assay. Titration of 8oxodGTP and dGTP nucleotides (1, 2, 5, 10, 20, and 50 μM). Incorporated 8oxoG (O, red) and radioactive T (green) in the extension products are indicated. A DNA recovery control (15mer) was included.

(B) Oligonucleotides used as telomerase substrates in (C) and (D) are aligned with the telomerase RNA (hTR) template (8oxoG [O, red], template [orange]).

(legend continued on next page)

attempt to counteract in vivo. However, the effects of ROS on the enzymatic activity of telomerase have not been examined to date. We chose to examine the effects of 8-oxoG on telomerase, because it is the most common DNA lesion caused by ROS. In vitro telomerase assays using purified human telomerase (Cristofari et al., 2007) revealed that 8-oxo-2′deoxyguanosine-5′-triphosphate (8oxodGTP) could be added onto a 5′-$(TTAGGG)_3$-3′ primer instead of dGTP (Figure 4A). However, extension was aborted after the addition of one or two telomeric repeats (Figure 4A, lanes 1–6). This therefore indicates that 8oxodGTP functions as chain terminator for telomerase. Analysis of the extension ladder further indicated that 8oxodGTP was incorporated efficiently into extension products when located opposite positions 46, 50, and 51 of the telomerase RNA (hTR) template but that 8oxodGTP was not tolerated opposite position 52 of hTR at the 3′ boundary of the template. Thus, 8oxodGTP blocked further extension when it was incorporated as first G in the 5′-TTAGGG-3′ sequence (Figure 4A). To better understand this effect, we tested DNA substrates terminating with 8-oxo-2′-deoxyguanosine and annealing opposite different positions of the telomerase RNA (hTR) template (Figures 4B and 4C); consistent with the results shown in Figure 4A, we found that the oxidized DNA substrates were extended efficiently when annealing opposite positions 50 of the telomerase RNA (hTR) template but that 8oxoG was not tolerated opposite position 52 of hTR at the 3′ boundary of the template (5′-$(TTAGGG)_2$TTAO-3′, O = 8oxoG; Figures 4B and 4C). Together, these data reveal that depending on the position within the telomeric repeat, 8oxoG severely impairs telomere extension by telomerase.

During semiconservative DNA replication by conventional DNA polymerases, 8oxoG mispairs with adenine, causing spontaneous mutations. To test if 8oxodGTP can mispair with adenine in the telomerase RNA template, we replaced dTTP by 8oxodGTP in a telomerase assay (Figure 4D). Though only short products were obtained, the extension pattern revealed increasing incorporation of 8oxodGTP opposite adenines of hTR as the concentration of 8oxodGTP in the reaction was raised. Thus, 8oxodGTP can be incorporated by telomerase instead of dTTP, thus causing telomeric DNA mutations.

Conclusions

ROS have been shown to promote telomere shortening (Ahmed et al., 2008; Sun et al., 2015; Wang et al., 2010), thereby accelerating cellular senescence (Forsyth et al., 2003); short telomeres may enhance oxidative stress (Sahin et al., 2011), activating checkpoint signaling, which stabilizes p53 and represses PGC-1α and PGC-1β. PGC-1α and PGC-1β repression compromises mitochondrial structure, causing leakage of oxygen radicals and thus enhancing oxidative stress in a positive-feedback mechanism (Sahin et al., 2011). Short telomeres also promote cardiac failure in Duchenne muscular dystrophy mouse models, and treatment with antioxidants significantly retards the onset of cardiac dysfunction, suggesting links among ROS, telomeres, and disease (Mourkioti et al., 2013). Loss of *PRDX1* in mice has also been linked to cancer development, hemolytic anemia, and shortened lifespan (Neumann et al., 2003), though the molecular mechanisms remain uncharacterized.

Telomeric DNA is sensitive to ROS-induced DNA damage. Here, we identify a key role for the antioxidant enzyme PRDX1 in preventing ROS-induced damage at telomeres. PRDX1 is likely to protect many macromolecules in the cytoplasm, reducing the cellular concentration of hydrogen peroxide. We propose that nuclear PRDX1 function contributes to a local ROS-protective shield for the telomeres through its association and enhanced concentration at telomeric chromatin and possibly other sites in the genome. Our data suggest that PRDX1 is not recruited to telomeres by shelterin components. Direct DNA binding of PRDX1 also seems not sufficient to explain chromatin recruitment, as PRDX1 displays only week affinity for DNA (data not shown). Therefore, other chromatin components may be involved. The enrichment with telomeres in S and G2 phases of the cell cycle and upon H_2O_2 treatment could be due to the involvement of DNA damage response pathways. Indeed, telomeric DNA may be especially vulnerable to ROS damage during DNA repair and replication. On the other hand, TRF1 and TRF2 may bind to telomeric DNA during DNA replication in a more dynamic fashion, facilitating the apparent shelterin-independent recruitment of PRDX1. Whatever the exact mechanism of recruitment, PRDX1 may reduce ROS-induced damage of proteins, RNA, DNA, and nucleotides at telomeres by diminishing the abundance of hydrogen peroxide near telomeres (Figure 4E). ROS-induced telomeric phosphate backbone breakage, such as that documented in this study, will cause stochastic telomere loss events if it is not repaired before chromosome segregation. 8oxoG-containing DNA templates impair replication fork progression during semiconservative DNA replication, leading to telomere loss when replication forks collapse. Here, we provide evidence that the extension of ROS-damaged truncated telomeres by telomerase can be strongly perturbed, as telomerase cannot extend certain 8oxoG-containing DNA substrates. Furthermore, incorporation of 8oxoG by telomerase creates chain-terminating chromosome ends that cannot be elongated. Thus, the consequence of ROS-induced damage of telomeric DNA inhibits the major chromosome-end-healing pathway (Gao et al., 2008). It will be important to dissect whether other antioxidant enzymes in addition to PRDX1 and DNA repair enzymes reduce the burden of ROS at telomeres and thus counteract genome instability, cancer, and cellular and organismal aging.

EXPERIMENTAL PROCEDURES

Cell Culture, Transfections, and Oxidative Stress

For SILAC labeling, HEK293E cells were grown for seven doublings in SILAC-modified InVitrus VP-6 medium. Transfections were done with Lipofectamine

(C) Same as (A) but using substrates containing terminal 8oxoG (O). Incorporated radioactive nucleotides (T/G) are in green.
(D) Same as (A) but performed in the absence of dTTP. 8oxodGTP was titrated from 2 to 50 μM.
(E) Model for PRDX1-mediated telomere protection. The shielding function of PRDX1 from ROS is schematically indicated by the umbrellas. See text for discussion.

2000 (Life Technologies). See Supplemental Experimental Procedures for details.

Centrifugal Elutriation

Cells were sorted using a Beckman JS5.0 elutriator rotor, fitted with a 40-mL separation chamber, in a Beckman J-6M centrifuge. Cells were harvested and fixed prior to elutriation. Cells were recovered by centrifugation, and a sample of each was analyzed by flow cytometry to determine which fractions should be pooled. See Supplemental Experimental Procedures for details.

Quantitative Telomeric Chromatin Isolation Protocol

QTIP was performed as previously described (Grolimund et al., 2013; Majerska et al., 2016) with several modifications indicated in Supplemental Experimental Procedures.

Mass Spectrometry Analysis

QTIP eluates were separated by 10% SDS-PAGE. Lanes were sliced into pieces, and proteins were reduced and alkylated before digestion with trypsin. Peptides were separated using a Dionex Ultimate 3000 rapid separation liquid chromatography (RSLC) nano ultra performance liquid chromatography (UPLC) system (Thermo Fisher Scientific) online connected with an Orbitrap Elite Mass Spectrometer (Thermo Fisher Scientific). See Supplemental Experimental Procedures for details.

Chromatin Immunoprecipitation

For HA and PRDX1 ChIP, cells were crosslinked with 1% formaldehyde (16%, methanol-free, Thermo Scientific) for 30 and 10 min at 25°C, respectively. Sonicated and diluted lysates were incubated with specific antibodies (anti-HA [ab9110, Abcam] and anti-PRDX1 [ab41906, Abcam]) and enriched on protein G Sepharose 4 fast flow at 4°C overnight. See Supplemental Experimental Procedures for details.

Immunoblots

Cell extracts were separated by PAGE. Standard immunoblot protocols were used with anti-PRDX1 (ab41906, Abcam) and anti-tubulin (T9026, Sigma-Aldrich) antibodies. See Supplemental Experimental Procedures for details.

Generation of *PRDX1*-Knockout Cell Lines

The *PRDX1* locus was targeted using CRISPR/Cas9 as described previously (Ran et al., 2013). Briefly, guide RNA target sequences (guide RNA [gRNA] 1, 5′-GCCACAGCTGTTATGCCAGA-3′; and gRNA 2, 5′-CAGCTGTTATGCCA GATGGT-3′ for knock out (KO)1 and KO2, respectively) were designed against exon 1 of *PRDX1* (NC_000001.11; gene ID 5052) using the Optimal CRISPR design tool (http://crispr.mit.edu/). The guide RNA target oligonucleotide and its complementary strand were annealed, cloned into a pSpCas9(BB)-2A-puro plasmid, and transfected into HT1080 or HCT116 cells. *PRDX1* mutant clones were screened by immunoblot analysis, and mutations in the *PRDX1* genes were detected by Sanger sequencing.

Menadione Treatment and Assessment of DNA Damage

Menadione treatment was performed on HT1080 or HCT116 cells in serum-free DMEM GlutMAX (Life Technologies) by addition of 1 mM menadione sodium bisulfite (Sigma-Aldrich). Cells were incubated for 30 min in incubator (37°C, 5% CO_2). Following menadione treatment, cells were washed with pre-warmed PBS and incubated in serum-free DMEM for 3 hr. DNA was isolated, restriction enzyme digested, and fractionated on 0.8% agarose containing 50 mM NaOH and 1 mM EDTA. Gels were transferred to Hybond N^+ membranes (Amersham). Southern hybridization was done as described previously (Grolimund et al., 2013), with probes indicated in the figure legends.

Telomerase Purification and Direct Telomerase Assay

Human telomerase was expressed and purified as described previously (Cristofari et al., 2007; Sauerwald et al., 2013). Direct telomerase assays were performed as described previously (Cristofari et al., 2007). See Supplemental Experimental Procedures for details.

ACCESSION NUMBERS

The accession number for the mass spectrometry proteomics data (Vizcaíno et al., 2014) reported in this paper is PRIDE: PXD002626.

SUPPLEMENTAL INFORMATION

Supplemental Information includes Supplemental Experimental Procedures and four figures and can be found with this article online at http://dx.doi.org/10.1016/j.celrep.2016.11.071.

AUTHOR CONTRIBUTIONS

E.A. performed the QTIP experiments. V.S. established and performed elutriation with assistance from E.A. PRDX1 chromatin immunoprecipitations were done by E.A. and W.A. W.A generated *PRDX1*-knockout cell lines with the assistance of S.R. Nick assays were performed by S.R. and W.A. based on protocols established by E.A. Telomerase assays were done by S.R. J.L., E.A., and V.S. wrote the paper.

ACKNOWLEDGMENTS

We thank F. Armand, R. Hamelin, D. Chappe, and M. Moniatte for mass spectrometry analysis and David Hacker, Sarah Thurnheer, and Larissa Grolimund for advice with cell cultures. Research in J.L.'s laboratory was supported by the Swiss National Science Foundation (SNSF) (grant agreement no. 166675), the SNSF-funded NCCR RNA and disease network (grant agreement no. 141735), an Initial Training Network (ITN) grant (CodeAge) from the European Commission's Seventh Framework Programme (grant agreement number 316354), the Swiss Cancer League (grant agreement no. KLS-3824-02-2016), and Ecole Polytechnique Fédérale de Lausanne (EPFL. Research in V.S.'s laboratory was supported by the SNSF (grant agreement no. 156769) and EPFL.

Received: September 14, 2016
Revised: November 4, 2016
Accepted: November 22, 2016
Published: December 20, 2016

REFERENCES

Ahmed, S., Passos, J.F., Birket, M.J., Beckmann, T., Brings, S., Peters, H., Birch-Machin, M.A., von Zglinicki, T., and Saretzki, G. (2008). Telomerase does not counteract telomere shortening but protects mitochondrial function under oxidative stress. J. Cell Sci. *121*, 1046–1053.

Banfalvi, G. (2008). Cell cycle synchronization of animal cells and nuclei by centrifugal elutriation. Nat. Protoc. *3*, 663–673.

Chae, H.Z., Robison, K., Poole, L.B., Church, G., Storz, G., and Rhee, S.G. (1994). Cloning and sequencing of thiol-specific antioxidant from mammalian brain: alkyl hydroperoxide reductase and thiol-specific antioxidant define a large family of antioxidant enzymes. Proc. Natl. Acad. Sci. USA *91*, 7017–7021.

Cristofari, G., Reichenbach, P., Regamey, P.O., Banfi, D., Chambon, M., Turcatti, G., and Lingner, J. (2007). Low- to high-throughput analysis of telomerase modulators with Telospot. Nat. Methods *4*, 851–853.

Doksani, Y., Wu, J.Y., de Lange, T., and Zhuang, X. (2013). Super-resolution fluorescence imaging of telomeres reveals TRF2-dependent T-loop formation. Cell *155*, 345–356.

Forsyth, N.R., Evans, A.P., Shay, J.W., and Wright, W.E. (2003). Developmental differences in the immortalization of lung fibroblasts by telomerase. Aging Cell *2*, 235–243.

Fumagalli, M., Rossiello, F., Clerici, M., Barozzi, S., Cittaro, D., Kaplunov, J.M., Bucci, G., Dobreva, M., Matti, V., Beausejour, C.M., et al. (2012). Telomeric DNA damage is irreparable and causes persistent DNA-damage-response activation. Nat. Cell Biol. *14*, 355–365.

Gao, Q., Reynolds, G.E., Wilcox, A., Miller, D., Cheung, P., Artandi, S.E., and Murnane, J.P. (2008). Telomerase-dependent and -independent chromosome healing in mouse embryonic stem cells. DNA Repair (Amst.) *7*, 1233–1249.

Grolimund, L., Aeby, E., Hamelin, R., Armand, F., Chiappe, D., Moniatte, M., and Lingner, J. (2013). A quantitative telomeric chromatin isolation protocol identifies different telomeric states. Nat. Commun. *4*, 2848.

Haendeler, J., Hoffmann, J., Brandes, R.P., Zeiher, A.M., and Dimmeler, S. (2003). Hydrogen peroxide triggers nuclear export of telomerase reverse transcriptase via Src kinase family-dependent phosphorylation of tyrosine 707. Mol. Cell. Biol. *23*, 4598–4610.

Loor, G., Kondapalli, J., Schriewer, J.M., Chandel, N.S., Vanden Hoek, T.L., and Schumacker, P.T. (2010). Menadione triggers cell death through ROS-dependent mechanisms involving PARP activation without requiring apoptosis. Free Radic. Biol. Med. *49*, 1925–1936.

Majerska, J., Redon, S., and Lingner, J. (2016). Quantitative telomeric chromatin isolation protocol for human cells. Methods, Published online August 9, 2016. http://dx.doi.org/10.1016/j.ymeth.2016.08.003.

Miller, K.M., Rog, O., and Cooper, J.P. (2006). Semi-conservative DNA replication through telomeres requires Taz1. Nature *440*, 824–828.

Mourkioti, F., Kustan, J., Kraft, P., Day, J.W., Zhao, M.M., Kost-Alimova, M., Protopopov, A., DePinho, R.A., Bernstein, D., Meeker, A.K., and Blau, H.M. (2013). Role of telomere dysfunction in cardiac failure in Duchenne muscular dystrophy. Nat. Cell Biol. *15*, 895–904.

Neumann, C.A., Krause, D.S., Carman, C.V., Das, S., Dubey, D.P., Abraham, J.L., Bronson, R.T., Fujiwara, Y., Orkin, S.H., and Van Etten, R.A. (2003). Essential role for the peroxiredoxin Prdx1 in erythrocyte antioxidant defence and tumour suppression. Nature *424*, 561–565.

Oikawa, S., and Kawanishi, S. (1999). Site-specific DNA damage at GGG sequence by oxidative stress may accelerate telomere shortening. FEBS Lett. *453*, 365–368.

Ong, S.E., and Mann, M. (2007). Stable isotope labeling by amino acids in cell culture for quantitative proteomics. Methods Mol. Biol. *359*, 37–52.

Perkins, A., Nelson, K.J., Parsonage, D., Poole, L.B., and Karplus, P.A. (2015). Peroxiredoxins: guardians against oxidative stress and modulators of peroxide signaling. Trends Biochem. Sci. *40*, 435–445.

Ran, F.A., Hsu, P.D., Wright, J., Agarwala, V., Scott, D.A., and Zhang, F. (2013). Genome engineering using the CRISPR-Cas9 system. Nat. Protoc. *8*, 2281–2308.

Sahin, E., Colla, S., Liesa, M., Moslehi, J., Müller, F.L., Guo, M., Cooper, M., Kotton, D., Fabian, A.J., Walkey, C., et al. (2011). Telomere dysfunction induces metabolic and mitochondrial compromise. Nature *470*, 359–365.

Sauerwald, A., Sandin, S., Cristofari, G., Scheres, S.H., Lingner, J., and Rhodes, D. (2013). Structure of active dimeric human telomerase. Nat. Struct. Mol. Biol. *20*, 454–460.

Sfeir, A., and de Lange, T. (2012). Removal of shelterin reveals the telomere end-protection problem. Science *336*, 593–597.

Sfeir, A., Kosiyatrakul, S.T., Hockemeyer, D., MacRae, S.L., Karlseder, J., Schildkraut, C.L., and de Lange, T. (2009). Mammalian telomeres resemble fragile sites and require TRF1 for efficient replication. Cell *138*, 90–103.

Sun, L., Tan, R., Xu, J., LaFace, J., Gao, Y., Xiao, Y., Attar, M., Neumann, C., Li, G.M., Su, B., et al. (2015). Targeted DNA damage at individual telomeres disrupts their integrity and triggers cell death. Nucleic Acids Res. *43*, 6334–6347.

Vannier, J.B., Pavicic-Kaltenbrunner, V., Petalcorin, M.I., Ding, H., and Boulton, S.J. (2012). RTEL1 dismantles T loops and counteracts telomeric G4-DNA to maintain telomere integrity. Cell *149*, 795–806.

Vizcaíno, J.A., Deutsch, E.W., Wang, R., Csordas, A., Reisinger, F., Ríos, D., Dianes, J.A., Sun, Z., Farrah, T., Bandeira, N., et al. (2014). ProteomeXchange provides globally coordinated proteomics data submission and dissemination. Nat. Biotechnol. *32*, 223–226.

von Zglinicki, T. (2002). Oxidative stress shortens telomeres. Trends Biochem. Sci. *27*, 339–344.

Wang, Z., Rhee, D.B., Lu, J., Bohr, C.T., Zhou, F., Vallabhaneni, H., de Souza-Pinto, N.C., and Liu, Y. (2010). Characterization of oxidative guanine damage and repair in mammalian telomeres. PLoS Genet. *6*, e1000951.